Vol. 23 • No. 43 • November 16 • 2011

www.advmat.de

ADVANCED MATERIALS

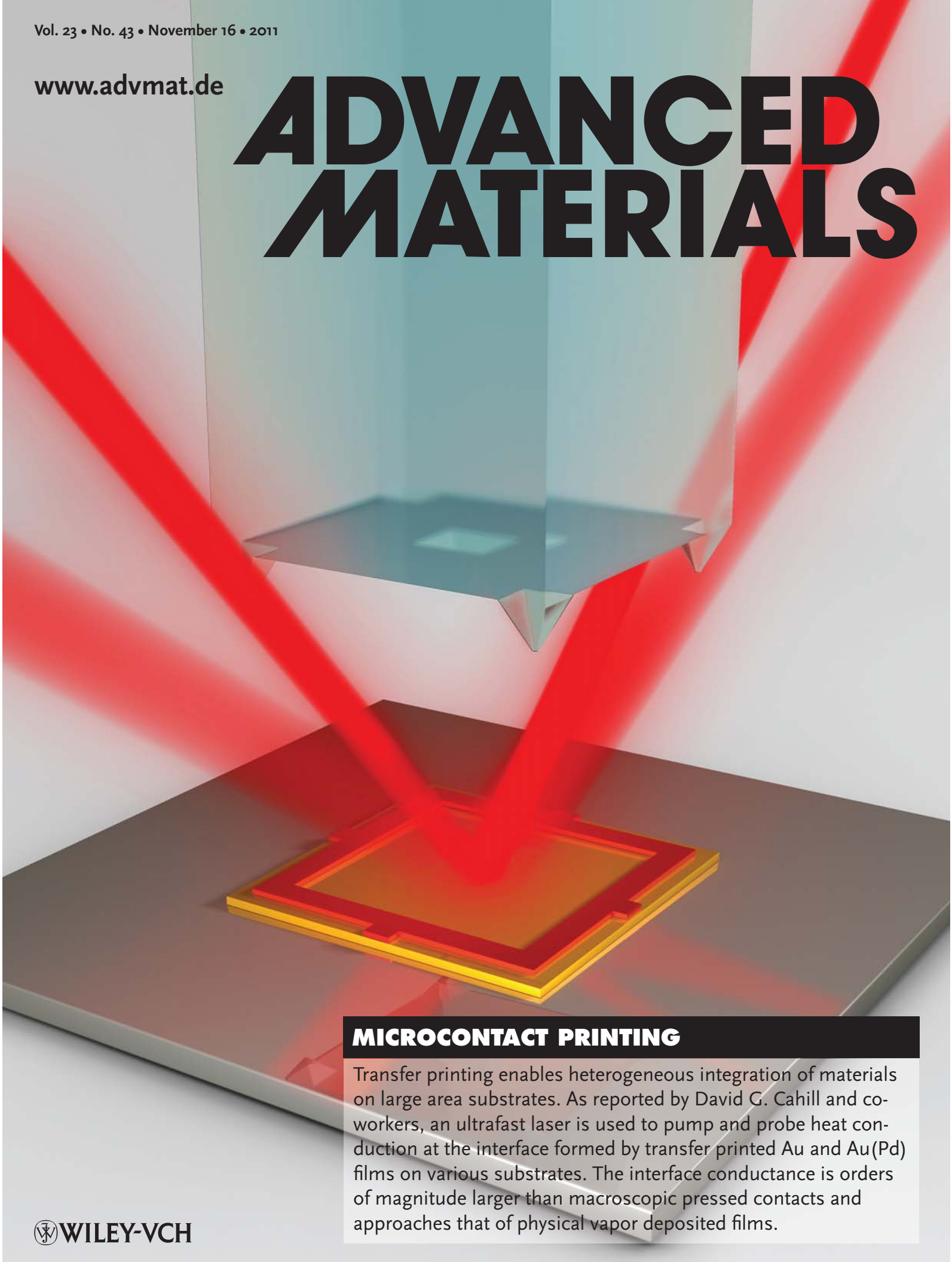

MICROCONTACT PRINTING

Transfer printing enables heterogeneous integration of materials on large area substrates. As reported by David G. Cahill and co-workers, an ultrafast laser is used to pump and probe heat conduction at the interface formed by transfer printed Au and Au(Pd) films on various substrates. The interface conductance is orders of magnitude larger than macroscopic pressed contacts and approaches that of physical vapor deposited films.

WILEY-VCH

ADVANCED MATERIALS
www.advmat.de

www.MaterialsViews.com

Interfacial Thermal Conductance of Transfer-Printed Metal Films

Dong-Wook Oh, Seok Kim, John A. Rogers, David G. Cahill, and Sanjiv Sinha*

Deterministic assembly of microdevices by transfer-printing is an advanced manufacturing technology that enables the heterogeneous integration of disparate materials on large-area substrates.[1–5] All active electronic devices generate heat as a byproduct of their operation and thermal management of transfer-printed assemblies must be a consideration whenever the heat flux is large. While the thermal conductivities of most materials used in microelectronics are well known, the thermal conductance of interfaces formed by transfer-printing is unknown. We report studies of the thermal conductance of interfaces formed by transfer-printing of Au and Au(Pd) alloy thin films, 100 μm × 100 μm in area and 100 nm thick, on amorphous SiO_2, hydrogen-terminated Si(001), and single-crystal Al_2O_3 substrates. We find that the thermal conductance G_t of transfer-printed interfaces spans a relatively small range, $10 < G_t < 40\ \mathrm{MWm^{-2}K^{-1}}$ despite significant differences in the thermal conductivity of the substrates and interfaces roughness. These values of G_t are smaller than the conductance of interfaces formed by physical vapor deposition but orders of magnitude larger than the conductance of pressed contacts between macroscopic polished surfaces. The relatively small thermal resistance of transfer-printed interfaces will not create a significant thermal management problem in most applications of transfer-printing but will be a concern in high-power technologies that involve extremely large heat fluxes, >10 kW cm^{-2}.

The thermal conductance G of interfaces formed by physical vapor deposition of metal films on dielectric substrates has been studied extensively. G is the transport coefficient that relates the heat flux J_Q to the temperature drop ΔT at an interface, $J_Q = G\Delta T$. The observed values span a large range, from a low conductance of $G \approx 10\ \mathrm{MWm^{-2}K^{-1}}$ for Bi deposited on hydrogen-terminated diamond[6] to a high conductance[7] of $G \approx 700\ \mathrm{MWm^{-2}K^{-1}}$ for epitaxial TiN/MgO. Often, the thermal conductance of interfaces formed by physical vapor deposition is reasonably well understood based on the mismatch of vibrational densities of states between the two materials that make up the interface. Controversial issues remain, however, including the role of anharmonicity in enhancing heat transfer between highly dissimilar materials[6] and the role of weak interfacial bonding in suppressing heat transfer far below the values predicted by conventional theory.[8]

The thermal conductance of mechanically-joined materials has also been extensively studied because of their great practical importance in a wide variety of engineering systems.[9,10] The "thermal contact conductance" of joints is many orders of magnitude of smaller than the thermal conductance of interfaces formed by physical vapor deposition. Low values of thermal contact conductance, $G \sim 0.1\ \mathrm{MWm^{-2}K^{-1}}$, are also observed in micro-mechanical actuators.[11,12] By contrast, little is known about the thermal conductance of interfaces formed by transfer printing of a thin film on the types of relatively smooth substrates used in device manufacturing. Prior experimental work is limited to data for stiction-failed Si microcantilevers[13] and Au films transferred to GaAs substrates using alkane-dithiols as an adhesion layer.[14] A thin film will elastically deform to accommodate roughness on large lengths scales but interface roughness on short lengths will remain unless a large pressure is applied. The effects of the remaining nanoscale interface roughness on thermal transport have recently been studied theoretically by Persson.[15] This interface roughness suppresses the true area of contact to an extent that is difficult to predict: i.e., the true area of contact between the film and substrate A is an unknown fraction of the nominal contact area, A_0.[16]

Our experiments show that even for moderately rough transfer-printed interfaces, rms roughness ≈2 nm, the thermal conductance G_t of a transfer-printed interface is surprisingly large, $10 < G_t < 20\ \mathrm{MWm^{-2}K^{-1}}$. This interface conductance is only a factor of ≈4 smaller than G_S for Au sputter deposited SiO_2. We hypothesize that water adsorbed on the substrate and film surfaces from the ambient air generates sufficient capillary forces[17,18,19] to create a true area of contact A that is significant fraction of the nominal area A_0; and that the observed value of G_t reflects the intrinsic thermal conductance of the atomically-bonded bonded interface, G, scaled by the fractional area A/A_0, $G_t \approx G(A/A_0)$. Capillarity provides the force needed to pull the film and substrate together and create significant A/A_0 but the nanoscale water bridges themselves do not dominate the interfacial heat transport.

Our experiments employed two types of metal films, pure Au and a dilute Au(Pd) alloy with 5 at% Pd; and 3 substrates, SiO_2, sapphire, and hydrogen-terminated Si. (We chose the Au(Pd) alloy films for this study because the addition of a small amount

Dr. D.-W. Oh,[+,++] Dr. S. Kim,[+] Prof. J. A. Rogers, Prof. D. G. Cahill
Department of Materials Science and Engineering
Materials Research Laboratory
University of Illinois
Urbana, Illinois 61801, USA
E-mail: d-cahill@illinois.edu
Prof. S. Sinha
Department of Mechanical Science and Engineering
University of Illinois
Urbana, Illinois 61801, USA
[+]D.-W.O. and S.K. contributed equally to this work.
[++]Present Address: Department of Thermal Systems, Korea Institute of Machinery and Materials, Daejon 305-343, Korea

DOI: 10.1002/adma.201102994

© 2011 WILEY-VCH Verlag GmbH & Co. KGaA, Weinheim

Pd to Au dramatically improves the optical properties of Au for time-domain thermoreflectance measurements.[20]) To prepare Au films for transfer printing, we deposited 100 nm of Au by magnetron sputtering on 1.1 μm thick thermally grown SiO_2 as the sacrificial layer. We found that we could not use SiO_2 as a sacrificial layer for Au(Pd) alloy films because Au(Pd) films are damaged by an HF solution; instead, we used a 1 μm thick layer of sputter-deposited Cr as the sacrificial layer for Au(Pd). Au(Pd) alloy films were deposited on the Cr sacrificial layer by magnetron sputter deposition from an alloy target.

We characterized the surface morphology of the sacrificial layers and the substrates using atomic force microscopy. We assume that the morphology of the transfer-printed metal film is similar to morphology of the corresponding sacrificial layer. The height-difference correlation function $g(\rho)$ is a real-space, statistical measure[21] of surface morphology that provides more extensive information about the morphology than a simple measurement of the rms roughness. $g(\rho) = \langle (h_i - h_j)^2 \rangle$, where h_i, h_j are the heights of the surface at position i and j, respectively; ρ is the distance between surface points i and j; and the brackets denote an average over many pairs of surface points i and j. When a surface morphology is dominated by a narrow distribution of in-plane length-scales centered at ξ, $[g(\rho)]^{1/2}$ increases linearly with ϱ for $\varrho < \xi$ and is approximately constant and equal to $\sqrt{2}$ times the rms roughness for $\varrho > \xi$. The in-plane length scale ξ of the Cr sacrificial layer, and the SiO_2 and Al_2O_3 receiving substrates are $\xi \approx 30$, 10, and 70 nm, respectively. The length scale ξ for the Si:H receiving substrate is not as well defined, see **Figure 1**. On short length scales, $\varrho < \xi$, $[g(\rho)]^{1/2}/\rho$ is nearly constant and provides a measure of the rms slope of the surface morphology. $[g(\rho)]^{1/2}/\rho$ for the SiO_2 and Al_2O_3 substrates, and the Cr sacrificial layer are 0.021, 0.016, and 0.12, respectively.

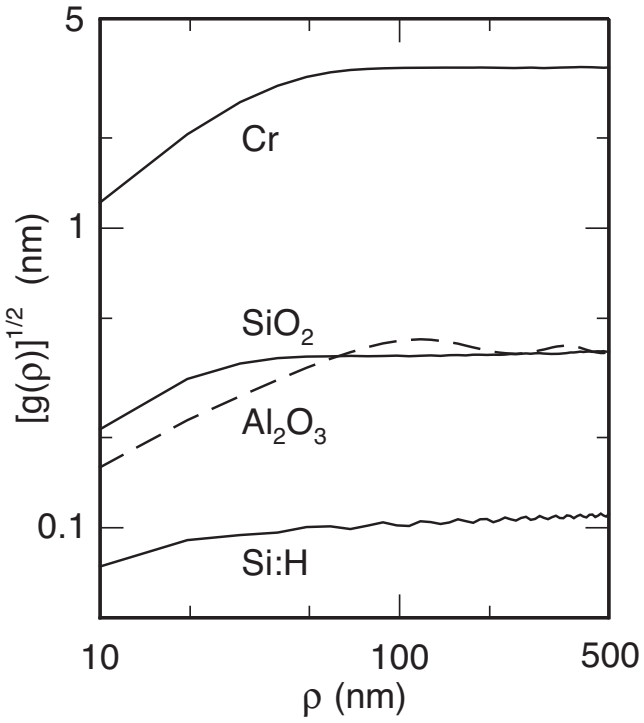

Figure 1. Square root of the height difference correlation function of the surface morphology of the sacrifical layers (amorphous SiO_2, Cr) and the receiving substrates (amorphous SiO_2, single crystal Al_2O_3, and hydrogen-terminated Si).

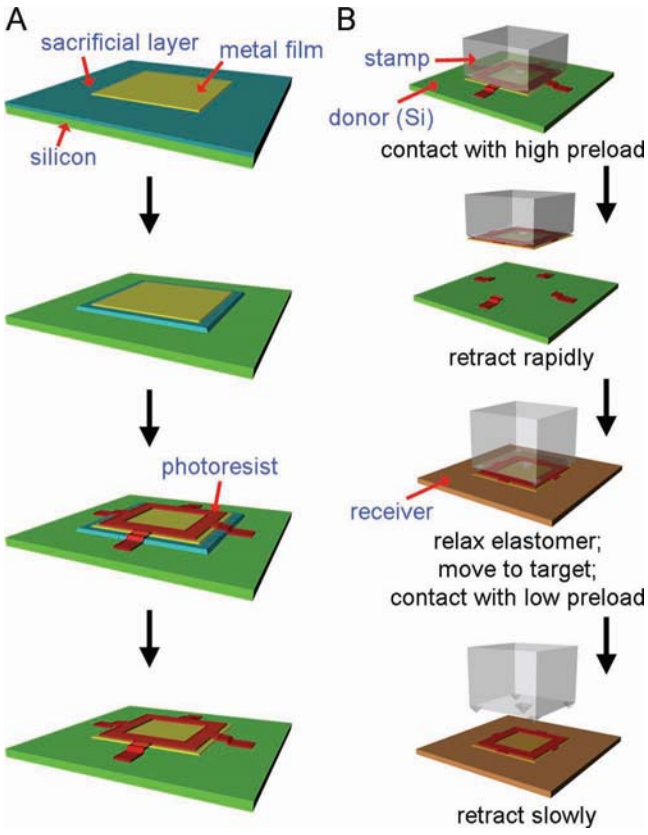

Figure 2. Illustration of the method of sample preparation. (a) Process flow for the fabrication of the transfer-printable metal film. From top to bottom: deposition and patterning of the 100 μm × 100 μm metal film on a sacrificial layer; patterning of the sacrificial layer to an area of 120 μm × 120 μm; patterning of photoresist anchors and frame; releasing of the metal film by etching the remaining sacrificial layer. (b) Process flow for transfer-printing.

The samples are assembled using the process flow illustrated in **Figure 2**. We pattern the metal films to a $100 \times 100\ \mu m^2$ followed by patterning of the sacrificial layer to 100 μm × 120 μm. Photoresist (AZ5214) is spun on the sample and patterned to form four anchors and a "picture frame" that supports thin metal films after the sacrificial layer is etched and the metal film is released from the substrate. SiO_2 sacrificial layers are removed by etching in a concentrated HF solution; Cr sacrificial layers are removed by etching in a commercially available Cr etchant. Pressing the stamp against the metal film on a donor substrate collapses the central area between the microtips and creates nearly full contact between the stamp and the metal film.[1] In this configuration, the adhesion between the stamp and the metal film is high. Rapidly retracting the stamp detaches the metal film from the donor substrate. Elastic restoring forces subsequently pull the stamp back in its original geometry. In this configuration, the strength of adhesion

© 2011 WILEY-VCH Verlag GmbH & Co. KGaA, Weinheim

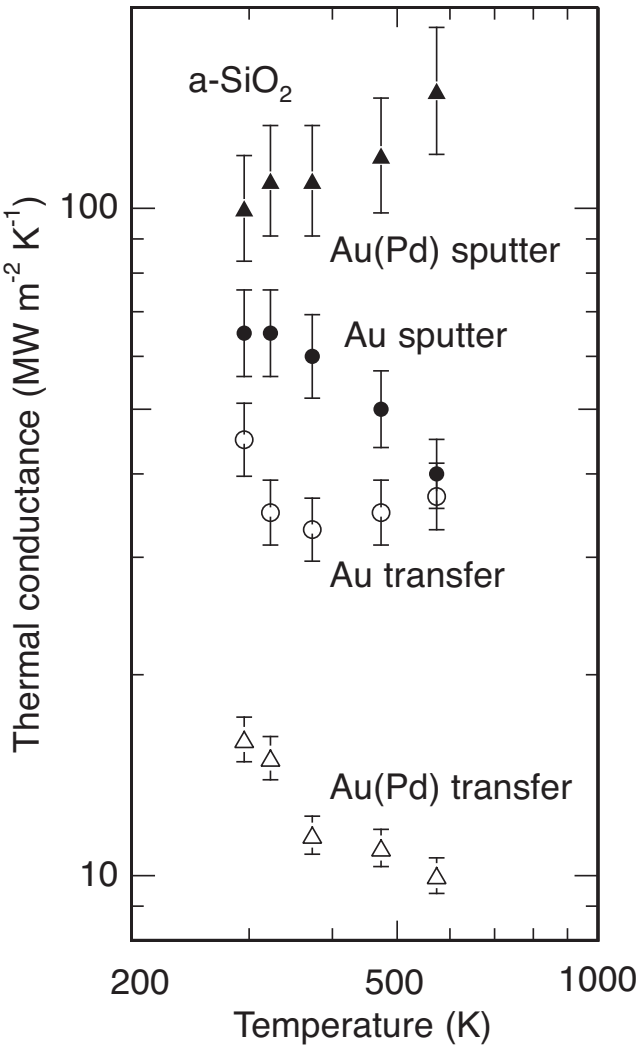

Figure 3. The thermal conductance of interfaces formed by sputter deposition and by transfer-printing Au and Au(Pd) metal films on amorphous SiO_2 receiving substrates. Solid symbols are for sputter-deposited films and open symbols are for transfer-printed films; circles are for Au films and triangles are for Au(Pd) alloys films. The SiO_2 substrates are thermally grown oxide, 1.1 μm thick, on a Si substrate. Error bars reflect experimental uncertainties in G that propagate from uncertainty in the thickness of the metal films. The data are measured as a function of temperature while heating the sample. The drop in G of the transfer-printed Au/SiO_2 interface with increasing temperature is not reversible.

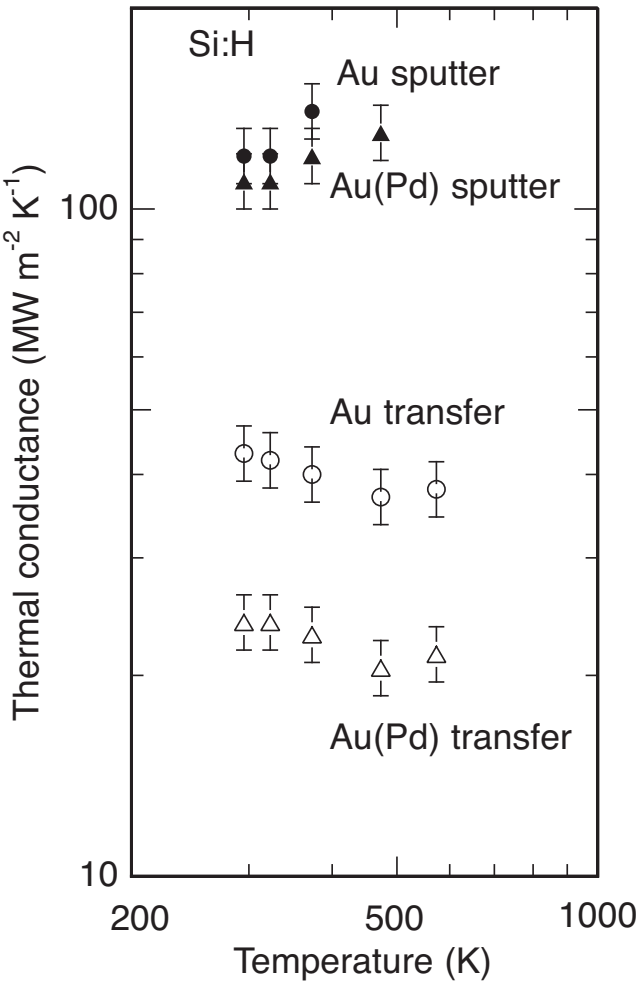

Figure 4. The thermal conductance of interfaces formed by physical vapor deposition and transfer-printing of Au and Au(Pd) alloy metal films on hydrogen-terminated Si(001). The highest temperature data points for sputter deposited films could not be measured because of solid-state reactions between the Au-containing films and the Si substrate. The transfer-printed films, on the other hand, were stable up to $T = 400$ °C.

between the stamp and the metal film is low because the area of contact between the microtips and the metal film is small.[1] The transfer-printing process is completed by gently contacting the film to a receiver substrate and then retracting the stamp.

We use time-domain thermoreflectance (TDTR), a pump-probe optical technique, to measure the thermal conductance of transfer-printed and sputter-deposited interfaces.[22,6] Experimental results for SiO_2, hydrogen-terminated Si(001), and Al_2O_3 receiving substrates are plotted in **Figures 3**, **4**, and **5**, respectively. In general, the thermal conductance of interfaces formed by transfer printing, G_t, are lower than the conductance of interfaces formed by sputter deposition, G_S, but the differences are surprisingly modest. In the case of Au(Pd), the ratio G_t/G_S ranges between $G_t/G_S \approx 0.25$ for Al_2O_3 receiving substrates and $G_t/G_S \approx 0.1$ for SiO_2 receiving substrates. In the case of Au, $G_t/G_S > 0.5$ for SiO_2 receiving substrates and $G_t/G_S \approx 0.2$ for Si:H receiving substrates.

For sputter-deposited Au and Au(Pd) films, G_S tends to increase with increasing temperature. This observation is counter to the predictions of models for interface thermal conductance that only consider two-phonon scattering processes, i.e., the elastic exchange of energy between the vibrational modes on the two sides of the interface. We have previously argued that this temperature dependence is a signature of three-phonon interactions, i.e., anharmonic interactions between two phonons in a low Debye temperature materials with one phonon in a high Debye temperature substrate.[6] These effects of anharmonicity have also been observed in computer simulations.[8] The reduction in G_S of Au sputter-deposited on SiO_2 with increasing temperature, see Figure 3, is not reversible and is apparently caused by changes in the interface contact area

© 2011 WILEY-VCH Verlag GmbH & Co. KGaA, Weinheim

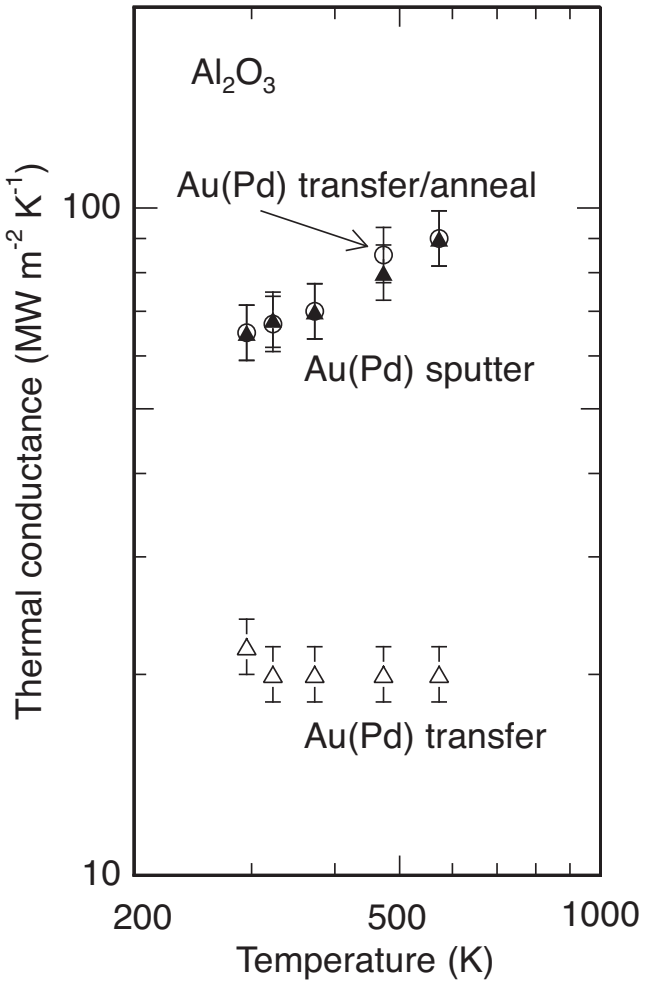

Figure 5. The thermal conductance of transfer-printed interfaces of Au(Pd) on sapphire before (open triangles) and after annealing in forming gas (3 at% H_2 in Ar) at 1100 °C for 1 hour (open circles). Data for a Au(Pd) deposited directly on sapphire by magnetron sputtering (filled triangles) are included for comparison and are essentially identical to the data for the interface formed by annealing the transfer-printed film.

created by the relatively large thermal expansion mismatch between Au and the SiO_2/Si substrate.

As expected, we can reproduce the behavior of sputtered films by annealing a transfer-printed film at sufficiently high temperatures, see Figure 5. In this example, annealing of the Au(Pd) film in H_2/Ar presumably reduces surface oxides and facilitates mass transport at the interface so that the Au(Pd) transfer-printed film forms an intimate contact with the sapphire substrate.

Our TDTR measurements are performed in air but we do not believe that heat transfer by gas molecules can contribute significantly to the transfer of heat between the metal film and substrate when $G_t > 1\ \mathrm{MWm^{-2}K^{-1}}$. The thermal conductance of an air gap of thickness smaller than the molecular mean-free-path l is approximately $G_a \approx \alpha\Lambda_a/l$ where α is a thermal accommodation coefficient and Λ_a is the thermal conductivity of air. Even at the upper limit of $\alpha = 1$, $G_a < 0.1\ \mathrm{MWm^{-2}K^{-1}}$ and negligible on the scale of G_t that we observe.

We do not observe a dependence of G_t on the existence of polar vibrational modes in the substrates. Al_2O_3 and SiO_2 have infrared active vibrational modes but Si does not. Thus, mechanisms for heat transport that are based on coupling of electronic excitations in the metals films with the vibrational modes of the substrate[23,24,15] do not appear to be important in our experiments. (We note, however, that this conclusion is difficult to make quantitative because the lack of infrared active modes at long wavelengths does not necessarily exclude the possibility of such coupling on length-scales comparable to atomic spacings.[23] Also, the vibrational states of adsorbed water will couple to the electronic states of the metal film to a degree that is difficult to quantify.) The weak temperature dependence of G_t provides additional evidence that near-field radiative heat transfer[24,15,25] is not significant. The high frequency optical phonons of SiO_2 and Al_2O_3 that are presumably most important for near-field radiative transport are not fully thermally excited at room temperatures; near-field radiative heat transport involving these modes should therefore increase strongly with temperature.

Having ruled out heat transport by air conduction and near-field electromagnetic radiation, we conclude that G_t is controlled by the vibrational states of the film and substrate. Data for transfer-printed films, G_t, do not, however, show a systematic dependence on the thermal conductivity of the substrate. (The thermal conductivity of SiO_2, $\Lambda = 1.3\ \mathrm{Wm^{-1}K^{-1}}$ is a factor 25 times smaller than Al_2O_3 and a factor of 100 times smaller than Si.) This result is expected if the spatial extent d of the regions of intimate contact between film and substrate are small compared to the Kapitza length, $L_K = \Lambda/G$, of both the substrate and film. If we assume $G = 60\ \mathrm{MWm^{-2}K^{-1}}$ for a Au/dielectric interface, the smallest value of L_K for our combination of materials is $L_K \approx 20$ nm for SiO_2 receiving substrates. The lateral length scale ξ of the surface morphology provides an approximate upper bound on d: for SiO_2, $d < 30$ nm and the upper bound is comparable to L_K. If, on the other hand, the finite thermal conductance of material interfaces is neglected, i.e., the limit $L_K = 0$, then the thermal conductance of a rough interface is expected to have a strong dependence on Λ.[15] The fact that G_t is approximately the same on all three substrates suggests instead that d is comparable to or smaller than L_K for all cases we have studied.

Data in Figures 3, 4, and 5, were collected while heating the samples. In most cases G_t decreases slightly with initial heating to 100 °C and then remains nearly constant up to 300 °C. We attribute these changes in conductance to the presence of liquid water at the interfaces that contributes to heat transfer[15] at room temperature and is mostly removed at elevated temperatures. The small lateral dimensions of the metal films, 100 μm × 100 μm, facilitates the escape of water and the small quantiy of volatile organic contaminates[26] that condense on the surfaces during the short elapsed time between preparation of the substrates and transfer-printing the metal film. We do not know how quickly water can escape from the narrow interface but the diffusion time τ of water on a length scale of $L = 50$ μm provides some insight: $\tau = L^2/(2D)$, where $D = 2 \times 10^{-5}\ \mathrm{cm^2s^{-1}}$ is the diffusion coefficient of water. $\tau \sim 1$ s, a time-scale that is a factor of $\sim$1000 shorter the time required to collect the temperature dependent TDTR data. Furthermore, we note that

© 2011 WILEY-VCH Verlag GmbH & Co. KGaA, Weinheim

the vapor pressure of water at 300 °C is nearly 100 atm, and that 300 °C closely approaches the temperature of the critical point of water, 374 °C. At such high temperatures, the surface tension of water is strongly reduced.

Heat transfer between the transfer-printed film and substrate is controlled by the interfacial thermal conductance of the small area of intimate contact. The relatively large values of G_t/G_S that we observe imply that the true area of contact A is a significant fraction of the nominal contact area A_0, $A/A_0 > 0.1$. A detailed discussion of the mechanics[16] needed to quantitatively describe A/A_0 of a rough interface is beyond the scope of our experimental study but we point out that it is unlikely that intrinsic van der Waals attraction[27] and the pressure used to assembly the sample are sufficient to generate a A/A_0 ratio of this magnitude when the film and substrate are elastically stiff. We instead invoke capillary pressure[18] created by adsorbed water to explain the strong forces needed to create large A/A_0. At relative humidities near 50%, the equilibrium coverage of water on gold,[28] hydrophilic silicon dioxide,[29] and sapphire[30] is 1–3 monolayers. (The coverage of adsorbed water on our SiO_2 substrates, prepared by heating to 950 °C, is not known but we expect the water coverage to be smaller than the ≈1 nm layer reported in Ref. [29]; hydrogen-terminated Si is hydrophobic and the coverage of water is probably even smaller.) Persson[18] has shown that capillary effects are strongest when adsorbed water can just fill the empty spaces at the interface. Thus, small rms roughness produces stronger capillary pressure and enhances A/A_0. Small values of the mean slope of the surface will also enhance the true area of contact.[16]

In summary, we observe surprisingly large thermal conductance G_t at interfaces between-transfer printed metal films and a variety of relatively smooth substrates of the type used in device manufacturing. For the combinations of materials we studied, values for G_t are always >10% of the value of G_S for the corresponding interface formed by sputter-deposition. The weak dependence of G_t on the thermal conductivity and infrared optical properties of the substrate show that spreading thermal resistance and near-field radiative heat transfer are not important considerations. A typical value is $G_t \sim 20\,\mathrm{MWm^{-2}K^{-1}}$, equivalent to the thermal conductance of a ∼100 nm thick layer of an amorphous dielectric. Thus, while G_t is an important consideration at sub-micron length-scales for devices with extremely high heat flux, G_t will not usually be a limiting factor in the thermal management of more typical electronic devices assembled by transfer-printing.

Experimental Section

Elastomeric microtip stamps were fabricated by casting and curing elastomer PDMS (polydemethlysiloxane) (Sylgard 184, Dow Corning; 5:1 mixture of base to curing agent).[1] Five pyramidal pits were fabricated on a Si(100) wafer by photolithography and anisotropic wet chemical etching. An epoxy (SU-8 50, MicroChem Corp.; 100 μm thick) was spun on the patterned silicon wafer and a square 100 μm × 100 μm hole was formed in the epoxy layer using photolithography. A PDMS precursor was poured into the negative templates composed of the hole in the epoxy layer and the pyramidal pits, cured in an oven for one hour at 70 °C, and peeled from the template to form the finished microtip stamp.[1]

Prior to transfer-printing of the metal films, the SiO_2 and Al_2O_3 receiving substrates are first prepared by rapid thermal annealing at 950 °C to remove volatile contaminates. The hydrogen terminated Si(001) receiving substrates are prepared by treatment with a 7:1 buffered-oxide etch for 20 s.

In TDTR, the time evolution of surface temperature is measured through temperature-dependent changes in the reflectivity, i.e., the thermoreflectance. (The thermoreflectance of Au(Pd) is a factor of ≈3 larger than pure Au.[20]) We analyze the ratio of in-phase $V_{in}(t)$ and out-of-phase $V_{out}(t)$ variations in the intensity of the reflected probe beam at the modulation frequency f = 9.8 MHz of the pump beam as a function of delay time t between pump and probe.[22] The wavelength of the mode-locked Ti:sapphire laser is λ = 785 nm and the $1/e^2$ radius of both focused beams is 7 μm. We used average pump and probe powers of 90 and 10 mW for Au, and 54 and 26 mW for Au(Pd). Our TDTR approach has been thoroughly validated and extensively applied in studies of the thermal conductivity of thin films[31] and the thermal conductance G of interfaces.[7,6] Typically, the dominate source of experimental uncertainty is the thickness of the metal film; we measure the film thickness by picosecond acoustics. Sensitivity analysis and error propagation are discussed in Refs. [31] and [6].

Acknowledgements

This research was supported by the Advanced Research Projects Agency—Energy grant no. DE-AR0000041 ARRA. Experiments were carried out in the Laser and Spectroscopy Laboratory of the Materials Research Laboratory at the University of Illinois, which is partially supported by the U.S. Department of Energy under grant DEFG02-91-ER45439.

Received: August 4, 2011
Published online: October 4, 2011

[1] S. Kim, J. Wu, A. Carlson, S. H. Jin, A. Kovalsky, P. Glass, Z. Liu, N. Ahmed, S. Elgan, W. Chen, P. Ferreira, M. Sitti, Y. Huang, J. Rogers, *Proc. Natl. Acad. Sci. USA* **2010**, *107*, 17095.
[2] C. E. Packard, A. Murarka, E. Lam, M. A. Schmidt, V. Bulovi , *Adv. Mater.* **2010**, *22*, 1840.
[3] D.-H. Kim, J. Xiao, J. Song, Y. Huang, J. Rogers, *Adv. Mater.* **2010**, *22*, 2108.
[4] R.-H. Kim, D.-H. Kim, J. Xiao, B. H. Kim, S.-I. Park, B. Panilaitis, R. Ghaffari, J. Yao, M. Li, Z. Liu, V. Malyarchuk, D. G. Kim, A.-P. Le, R. G. Nuzzo, D. L. Kaplan, F. G. Omenetto, Y. Huang, Z. Kang, J. A. Rogers, *Nat. Mater.* **2010**, *9*, 929.
[5] H. Fang, M. Madsen, C. Carraro, K. Takei, H. S. Kim, E. Plis, S.-Y. Chen, S. Krishna, Y.-L. Chueh, R. Maboudian, A. Javey, *Appl. Phys. Lett.* **2011**, *98*, 012111.
[6] H.-K. Lyeo, D. G. Cahill, *Phys. Rev. B* **2006**, *73*, 144301.
[7] R. M. Costescu, M. A. Wall, D. G. Cahill, *Phys. Rev. B* **2003**, *67*, 054302.
[8] M. Hu, P. Keblinski, P. Schelling, *Phys. Rev. B* **2009**, *79*, 104305.
[9] B. Snaith, S. D. Probert, P. W. O'Callaghan, *Appl. Energy* **1986**, *22*, 31.
[10] T. Aikawa, W. O. Winer, *Wear* **1994**, *177*, 25.
[11] W.-B. Song, M. S. Sutton, J. J. Talghadera, *Appl. Phys. Lett.* **2002**, *81*, 1216.
[12] J. Cho, C. Richards, D. Bahr, J. Jiao, R. Richards, *J. Micromech. Microeng.* **2008**, *18*, 105012.
[13] S. T. Huxtable, D. G. Cahill, L. M. Phinney, *J. Appl. Phys.* **2004**, *95*, 2102.
[14] R. Y. Wang, R. A. Segalman, A. Majumdar, *Appl. Phys. Lett.* **2006**, *89*, 173113.
[15] B. Persson, B. Lorenz, A. Volokitin, *Eur. Phys. J. E* **2010**, *31*, 3.
[16] S. Hyun, M. O. Robbins, *Tribology Int.* **2007**, *40*, 1413.

© 2011 WILEY-VCH Verlag GmbH & Co. KGaA, Weinheim

[17] Y. Ando, *Tribology Lett.* **2005**, *19*, 29.
[18] B. N. J. Persson, *J. Phys.: Condens. Matter* **2008**, *20*, 315007.
[19] P. J. van Zwol, G. Palasantzas, J. T. M. De Hosson, *Phys. Rev. E* **2008**, *78*, 031606.
[20] Y. Wang, J. Y. Park, Y. K. Koh, D. G. Cahill, *J. Appl. Phys.* **2010**, *108*, 043507.
[21] J. Lapujoulade, *Surf. Sci. Rep.* **1994**, *20*, 195.
[22] D. G. Cahill, *Rev. Sci. Instrum.* **2004**, *75*, 5119.
[23] G. D. Mahan, *Phys. Rev. B* **2009**, *79*, 075408.
[24] S.-A. Biehs, J.-J. Greffet, *Phys. Rev. B* **2010**, *82*, 245410.
[25] G. D. Mahan, *Appl. Phys. Lett.* **2011**, *98*, 132106.
[26] M. P. Seah, S. J. Spencer, *J. Vac. Sci. Technol. A* **2003**, *21*, 345.
[27] F. W. DelRio, M. P. de Boer, J. A. Knapp, E. D. Reedy, Jr., P. J. Clews, M. L. Dunn, *Nat. Mater.* **2005**, *4*, 629.
[28] V. Tsionsky, E. Gileadi, *Langmuir* **1994**, *10*, 2830.
[29] A. Verdaguer, C. Weis, G. Oncins, G. Ketteler, H. Bluhm, M. Salmeron, *Langmuir* **2007**, *23*, 9699.
[30] H. A. Al-Abadleh, V. H. Grassian, *Langmuir* **2003**, *19*, 341.
[31] Y. K. Koh, S. L. Singer, W. Kim, J. M. O. Zide, H. Lu, D. G. Cahill, A. Majumdar, A. C. Gossard, *J. Appl. Phys.* **2009**, *105*, 5054303.

© 2011 WILEY-VCH Verlag GmbH & Co. KGaA, Weinheim